Neuromorphic model-based neural decoders for brain-computer interfaces: a comparative study

Yijie Weng[1], Yu Qi[2,3,4], Yueming Wang[5], Gang Pan[3,4]

[1]College of Biomedical Engineering & Instrument Science, Zhejiang University, Hangzhou, China

[2]MOE Frontier Science Center for Brain Science and Brain-Machine Integration, Zhejiang University, Hangzhou, China

[3]College of Computer Science and Technology, Zhejiang University, Hangzhou, China

[4]The State Key Lab of Brain-Machine Intelligence, Zhejiang University, Hangzhou, China

[5]Qiushi Academy for Advanced Studies, Zhejiang University, Hangzhou, China

{wengyj, qiyu, ymingwang, gpan}@zju.edu.cn

2024 IEEE Biomedical Circuits and Systems Conference (BioCAS) | 979-8-3503-5495-9/24/$31.00 ©2024 IEEE | DOI: 10.1109/BioCAS61083.2024.10798332

***Abstract*—Brain-computer interfaces that convert neural signals into control commands for external devices have demonstrated great potential in neural rehabilitation. Most recently, the growing demand for developing large-scale brain signal recording devices has highlighted the need for power-efficient neural signal processing. Neuromorphic computing models, implemented with chips, can provide ultra-low-cost computation of neural signals, facilitating brain-implantable devices. In our work, we evaluated the neural decoding ability of neuromorphic models in comparison with traditional neural decoding approaches. We found that neuromorphic model-based neural decoders showed high accuracy comparable to existing decoders while with significantly lower computational costs. Our results suggest the potential of using neuromorphic models for highly efficient computing with large-scale brain data.**

Keywords—spiking neural networks, brain-computer interface, neural decoding, neuromorphic

I. Introduction

Restoring arm and hand movements is a critical clinical outcome for paralyzed individuals. Brain-computer interfaces (BCIs) offer a promising tool for restoring motor functions. Preliminary studies have demonstrated that BCIs facilitate control over computer cursors [1] [2] [3] [4] [5]. Despite rapid progress, the design of BCI systems is still limited by accuracy and efficiency, posing a critical barrier.

The selection of an appropriate decoder greatly impacts the decoding accuracy in BCI systems. As a classic linear decoder, Kalman filter (KF) has been employed in BCI research [2] [6] [7] [8] [9]. However, considering non-stationary and non-linear properties in neural signals, classical linear decoders such as KF can only yield suboptimal decoding accuracy [10]. Deep learning methods have become popular in neural decoding tasks [11] [12] [13] [14] [15], however, due to their relatively high computational costs, deep learning methods are unsuitable for brain-implantable devices.

Inspired by the structure and mechanism of biological neural circuits, neuromorphic models are gaining attention in machine intelligence [16]. Spiking neural networks (SNNs), a type of neuromorphic model, have been applied in several fields [17] [18]. SNNs could potentially provide high computation accuracy and efficiency in the scenario of neural decoding [19]. They convey information via binary pulses across plastic synapses, naturally connecting with biological neurons. Moreover, the computational costs of SNNs can be ultra-low, incorporating with neuromorphic chips. Recent research has demonstrated the advantages of SNNs in neural decoding tasks [20] [21] [22]. However, whether SNN-based neuromorphic models are suitable for neural decoding is still to be explored.

This study conducts a comparative analysis of traditional neural decoding models and neuromorphic models within a neural decoding task. We compared these two types of decoders in terms of decoding accuracy and computational cost. Our findings reveal that neuromorphic model-based decoders achieve decoding accuracy comparable to traditional KF decoders while exhibiting lower computational costs. These results suggest that neuromorphic models could be effectively implemented in edge devices processing extensive brain data.

II. Methods

A. Neural Recordings and Behavioral Task

Neural recordings, obtained from a public dataset [23], were collected from the primary motor cortex of a Rhesus macaque engaged in a point-to-point reaching task. The task required the monkey to reach targets randomly positioned on an 8 × 8 grid. Successful target acquisition necessitated the monkey's fingertip to maintain contact with the target for at least 450 ms. Subsequent targets were introduced immediately following a successful reach, ensuring uninterrupted task progression. The position of the monkey's fingertip and the target location were recorded at a frequency of 250 Hz in two orthogonal directions, expressed in Cartesian coordinates and measured in millimeters. This investigation utilized velocity data derived from positional data through differentiation. Additionally, eight sessions of neural data were used for our study.

B. Signal Processing and Feature Extraction

For this research, the multi-unit activity (MUA) was extracted from the raw neural signals. MUA encompasses spikes identified via a threshold-crossing technique, which eliminates the need for spike sorting [24]. This approach captures spikes surpassing a set amplitude threshold, thereby including a broader range of neuronal activity. To further analyze these signals, a bin size of 100 ms was employed for feature extraction. These temporal windows were chosen to provide a comprehensive overview of the neural activity across different time scales. For traditional neural decoding models, the spike rate of each neuron was determined from the MUA data. For spiking models, max-pooling within each time bin was utilized to compile the spike input, referred to as spiking MUA. The analysis was restricted to neurons

exhibiting a spike rate exceeding 0.5 Hz, ensuring the dataset represented substantial neural activity.

C. Decoding Methods

In this comparative study, we evaluated the decoding accuracy and computational cost of classical decoders versus neuromorphic decoders in a neural decoding task. From classical decoders, we chose KF as the baseline decoder. From neuromorphic decoders, we selected Leaky integrate-and-fire (LIF) model, Synaptic model and Alpha model. Each of these decoders is briefly described below.

1) Classical Neural Decoding Model: The KF is one of the most popular algorithms and has been used as a neural decoding algorithm in several BCI studies [2] [6] [7] [8] [9]. In linear dynamic systems, the KF is an optimal estimator with Gaussian noise. We implemented the KF as described in Wu et al. [6]. Velocity was used as the state variable in the KF decoder.

2) Neuromorphic Neural Decoding Models: In our study, we employ several SNN models, each utilizing different types of spiking neurons while maintaining the same fully connected architecture. For the sake of convenience, we refer to each SNN model by the name of its respective spiking neuron (e.g., LIF model).

- **The LIF model**: The LIF model is derived from animal neuroscience experiments. Besides modeling the integrated current over time on the membrane, it also models the diffusion of ions that occurs through the membrane. With its biological plausibility, simplicity, and low computational cost, the LIF model has potential in neural decoding [25].
- **The synaptic model**: The synaptic model incorporates synaptic conductance variation into LIF neurons, which are capable of modeling intricate firing patterns. Moreover, the membrane potential of synaptic neurons increases gradually with input spikes, making spike timing differentiable with respect to the membrane potential [26].
- **The Alpha model:** The Alpha model is a type of spike-response model that uses alpha function as the predefined kernel. The alpha function allows for more intricate interactions between presynaptic inputs [27], which provides ability to decode the hand kinematics from neural signals.

D. Performance Evaluation and Metrics

1) Decoding Accuracy: The Root Mean Square Error (RMSE) was used to evaluate the magnitude of the decoding error between the actual and predicted trajectories. Pearson's Correlation Coefficient (CC) was utilized to gauge the relationship (i.e., shape similarity) between the actual and predicted hand kinematics.

2) Computational Cost: Floating point operations (FLOPs) were used to quantify the computational cost. A single FLOP might constitute an addition, subtraction, division, multiplication, or any operation involving a floating point number. Table III represents the computing process of FLOPs for each decoder, where n denotes the number of neurons in each session, h represents the number of units in the hidden state of neuromorphic models and o denotes the output dimension of decoders.

TABLE I. HYPERPARAMETER SEARCH SPACE FOR OPTIMIZING SNN DECODERS

Hyperparameter	Search space
Number of units	{100,125,⋯,225}
Epochs	{5,10,⋯,25}
Learning rate	{0.0003,0.001,0.003,0.005,0.01,0.03}

TABLE II. OPTIMIZED HYPERPARAMETERS FOR SNN DECODERS

Hyperparameter	LIF	Synaptic	Alpha
Number of units	150	125	100
Number of epochs	5	15	5
Learning rate	0.03	0.03	0.001

TABLE III. FLOPS FOR EACH MODEL IN EACH TIME STEP

Models	FLOPs
KF	$n^3 + 4o^3 + 4o^2n + 4n^2o + n^2 + o^2 + no + n - o$
LIF	$2nh + 2ho + 8h + 2n$
Synaptic	$2nh + 2ho + 9h + 2n$
Alpha	$2nh + 2ho + 9h + 2n$

III. RESULTS

A. Hyperparameter Optimization

In the development of neuromorphic decoders, hyperparameters such as the number of units, learning rate, and epochs were optimized.

Data from each recording session were divided into ten equal, non-overlapping segments. These segments were allocated into three sets: eight segments for training, one for validation, and one for testing. The decoders were trained using an RMSE loss function. A grid search approach was employed for hyperparameter optimization, aiming to minimize the average RMSE on the validation set. The hyperparameter search spaces are shown in Table I, while the refined hyperparameters for the neuromorphic decoders are detailed in Table II.

B. Neuromorphic Decoders Achieve High Decoding Accuracy Comparable to KF

The study compared offline hand velocity decoding using KF and neuromorphic decoders. As indicated in Table III, the decoding accuracy for each decoder was assessed, with the average RMSE and CC calculated across eight sessions. Notably, certain neuromorphic decoders, such as the LIF and Synaptic models, surpassed KF in decoding performance. Using KF as the baseline, the LIF model improved the average decoding performance by 20.9% in terms of RMSE and by 6.4% in terms of CC, while the Synaptic model enhanced the average decoding performance by 22.0% (RMSE) and 6.4% (CC).

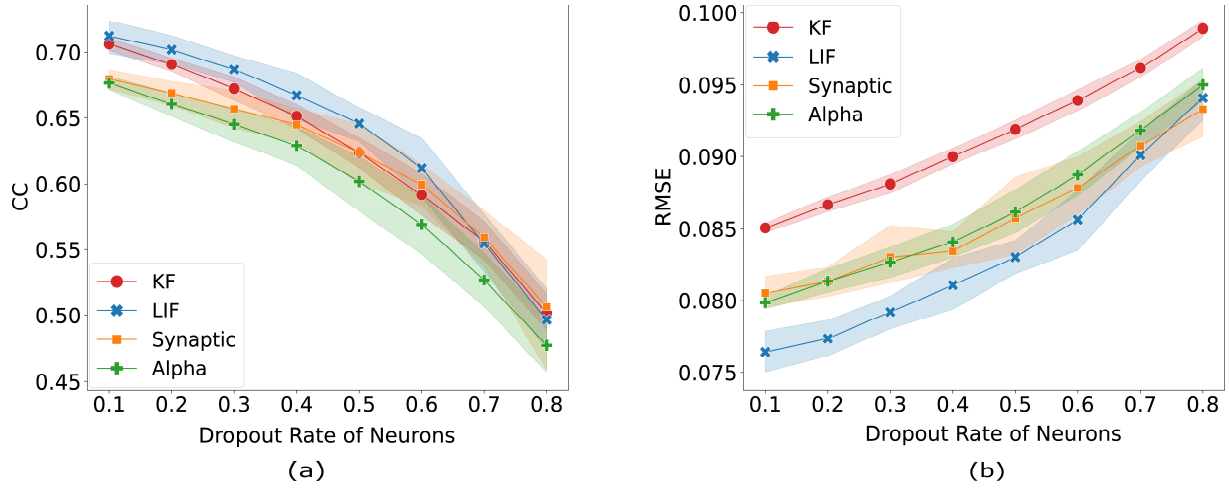

Fig. 1. Decoding accuracy among different decoders with randomly dropping neurons from neural signals, measured by (a) CC, (b) RMSE. Mean and standard variation are obtained by training on diverse neuron subsets with different dropout rates, repeated 20 times.

TABLE IV. DECODING ACCURACY AND COMPUTATIONAL COST OF THE CLASSICAL DECODER KF AND NEUROMORPHIC DECODERS

Model	RMSE	CC	FLOPs (normalized)
KF	0.091±0.027	0.626±0.102	1.0000
LIF	0.072±0.009	0.666±0.071	0.0029
Synaptic	0.071±0.007	0.666±0.040	0.0024
Alpha	0.079±0.009	0.592±0.074	0.0019

Furthermore, the study involved the random omission of neurons from the original neural signals to assess each decoder's performance. At the same dropout rate, the average decoding accuracy was determined by training 20 times on diverse subsets of neurons. Figure 1 depicted the decoding accuracy of KF and neuromorphic models at varying dropout rates. The neuromorphic decoders consistently achieved lower RMSE values across all dropout rates while maintaining comparable CC to the KF decoder. These findings suggested that neuromorphic models might possess an enhanced capability to manage noise and variability in neural signals and are potentially more adept at feature extraction.

C. *Neuromorphic Decoders Achieve Low Computational Cost Compared to KF*

To demonstrate that neuromorphic decoders achieved lower computational costs than KF, we computed their FLOPs as presented in Table III, adhering to the guidelines specified in [28]. Given that the output dimension o was two and the number of units in the hidden state h was fixed by predetermined hyperparameters, the FLOPs were directly correlated to the number of neurons n. As depicted in Table III, the FLOPs of KF increased cubically with the number of neurons, whereas the FLOPs of SNNs exhibited a linear relationship with the number of neurons. The normalized average FLOPs for each decoder during testing, per timestep for each session, were detailed in Column 4 of Table IV, benchmarked against the measurements from KF. The results in Table IV suggested that the computational efficiency of neuromorphic models surpassed that of the classical decoder KF. Specifically, the LIF model, Synaptic model, and Alpha model required 350.49×, 419.34× and 523.16× fewer FLOPs than KF, respectively. This result demonstrated the neuromorphic models' efficacy in conserving computational resources relative to KF, underscoring their viability for edge devices, such as brain-implantable systems.

IV. DISCUSSION

The present study offers an analysis of neuromorphic decoders in comparison to the classical KF decoder, focusing on decoding accuracy and computational cost. Our work underscores the potential of neuromorphic decoders in the hand kinematics neural decoding task.

On average over eight sessions, the neuromorphic decoders achieved decoding accuracy comparable to, and in some case surpassing, the KF decoder. Specifically, the LIF and Synaptic models showed improvements in RMSE and CC over the KF. These enhancements underscore the effectiveness of neuromorphic models in capturing the complex, non-linear dynamics inherent in neural signals. The superior performance of these models can be attributed to their biological plausibility and their ability to handle the non-stationary properties of neural data, which classical linear decoders like KF often struggle to address. Moreover, the robustness of neuromorphic decoders to variability and noise in neural signals was also evident from the analysis involving random neuron omissions. Neuromorphic models consistently achieved lower RMSE values across all dropout rates while maintaining comparable CC to the KF decoder. This indicates that the neuromorphic models have an enhanced capability to manage noise and variability in neural signals, making them more reliable for practical applications.

Our study also revealed that the computational cost, measured in FLOPs, for neuromorphic models is substantially lower than that of the KF decoder. This reduction can be attributed to the linear relationship between the number of neurons and FLOPs in neuromorphic models, as opposed to the cubic relationship in KF. This reduction in computational cost is particularly significant for the deployment of BCIs in real-world applications, where computational resources are often limited.

Despite the promising results, this study has several limitations. The analysis was conducted using a specific dataset and task, which may not fully capture the diversity of neural signals encountered in different contexts. Future research should explore the generalizability of these findings

across various datasets and tasks. Additionally, further optimization of neuromorphic models, including exploring different architectures and training algorithms, could potentially enhance their performance even further.

In conclusion, this study demonstrates the potential of neuromorphic decoders in neural decoding tasks, offering a compelling alternative to classical decoders like KF. The high decoding accuracy, robustness to signal variability, and low computational cost make neuromorphic models well-suited for practical BCI applications, paving the way for more efficient and effective restoration of motor functions in paralyzed individuals.

ACKNOWLEDGMENT

This work was supported by the STI 2030 Major Projects (2021ZD0200403), the Key Research and Development Program of Zhejiang Province in China (2023C03001), the Natural Science Foundation of China (62276228), and the Zhejiang Provincial Natural Science Foundation (LR24F020002). Corresponding author: Yu Qi.

REFERENCES

[1] L. R. Hochberg *et al.*, "Neuronal ensemble control of prosthetic devices by a human with tetraplegia," *Nature*, vol. 442, no. 7099, pp. 164–171, 2006.

[2] S.-P. Kim, J. D. Simeral, L. R. Hochberg, J. P. Donoghue, and M. J. Black, "Neural control of computer cursor velocity by decoding motor cortical spiking activity in humans with tetraplegia," *Journal of neural engineering*, vol. 5, no. 4, p. 455, 2008.

[3] J. Simeral, S.-P. Kim, M. Black, J. Donoghue, and L. Hochberg, "Neural control of cursor trajectory and click by a human with tetraplegia 1000 days after implant of an intracortical microelectrode array," *Journal of neural engineering*, vol. 8, no. 2, p. 025027, 2011.

[4] B. Jarosiewicz *et al.*, "Virtual typing by people with tetraplegia using a self-calibrating intracortical brain-computer interface," *Science translational medicine*, vol. 7, no. 313, pp. 313ra179-313ra179, 2015.

[5] Z. Wu, G. Pan, J. C. Principe, and A. Cichocki, "Cyborg intelligence: Towards bio-machine intelligent systems," *IEEE Intelligent Systems*, vol. 29, no. 06, pp. 2–4, 2014.

[6] W. Wu *et al.*, "Neural decoding of cursor motion using a Kalman filter," *Advances in neural information processing systems*, vol. 15, 2002.

[7] L. R. Hochberg *et al.*, "Reach and grasp by people with tetraplegia using a neurally controlled robotic arm," *Nature*, vol. 485, no. 7398, pp. 372–375, 2012.

[8] J. Zhuang, W. Truccolo, C. Vargas-Irwin, and J. P. Donoghue, "Decoding 3-D reach and grasp kinematics from high-frequency local field potentials in primate primary motor cortex," *IEEE Transactions on Biomedical Engineering*, vol. 57, no. 7, pp. 1774–1784, 2010.

[9] A. K. Bansal, W. Truccolo, C. E. Vargas-Irwin, and J. P. Donoghue, "Decoding 3D reach and grasp from hybrid signals in motor and premotor cortices: spikes, multiunit activity, and local field potentials," *Journal of neurophysiology*, vol. 107, no. 5, pp. 1337–1355, 2012.

[10] Y. Qi, B. Liu, Y. Wang, and G. Pan, "Dynamic ensemble modeling approach to nonstationary neural decoding in brain-computer interfaces," *Advances in neural information processing systems*, vol. 32, 2019.

[11] M. A. Schwemmer *et al.*, "Meeting brain–computer interface user performance expectations using a deep neural network decoding framework," *Nat Med*, vol. 24, no. 11, pp. 1669–1676, Nov. 2018, doi: 10.1038/s41591-018-0171-y.

[12] P.-H. Tseng, N. A. Urpi, M. Lebedev, and M. Nicolelis, "Decoding movements from cortical ensemble activity using a long short-term memory recurrent network," *Neural computation*, vol. 31, no. 6, pp. 1085–1113, 2019.

[13] N. Ahmadi, T. G. Constandinou, and C.-S. Bouganis, "Robust and accurate decoding of hand kinematics from entire spiking activity using deep learning," *Journal of Neural Engineering*, vol. 18, no. 2, p. 026011, 2021.

[14] S. Wen, A. Yin, T. Furlanello, M. G. Perich, L. E. Miller, and L. Itti, "Rapid adaptation of brain–computer interfaces to new neuronal ensembles or participants via generative modelling," *Nat. Biomed. Eng*, vol. 7, no. 4, pp. 546–558, Apr. 2023, doi: 10.1038/s41551-021-00811-z.

[15] J. Ye and C. Pandarinath, "Representation learning for neural population activity with Neural Data Transformers," Aug. 02, 2021, *arXiv*: arXiv:2108.01210. Accessed: Jun. 10, 2023. [Online]. Available: http://arxiv.org/abs/2108.01210

[16] K. Roy, A. Jaiswal, and P. Panda, "Towards spike-based machine intelligence with neuromorphic computing," *Nature*, vol. 575, no. 7784, pp. 607–617, 2019.

[17] Y. Hu, Q. Zheng, X. Jiang, and G. Pan, "Fast-SNN: fast spiking neural network by converting quantized ANN," *IEEE Transactions on Pattern Analysis and Machine Intelligence*, 2023.

[18] Y. Hu, H. Tang, and G. Pan, "Spiking deep residual networks," *IEEE Transactions on Neural Networks and Learning Systems*, vol. 34, no. 8, pp. 5200–5205, 2021.

[19] Y. Qi, J. Chen, and Y. Wang, "Neuromorphic computing facilitates deep brain-machine fusion for high-performance neuroprosthesis," *Frontiers in Neuroscience*, vol. 17, p. 1153985, 2023.

[20] J. Dethier, P. Nuyujukian, S. I. Ryu, K. V. Shenoy, and K. Boahen, "Design and validation of a real-time spiking-neural-network decoder for brain-machine interfaces," *J Neural Eng*, vol. 10, no. 3, p. 036008, Jun. 2013, doi: 10.1088/1741-2560/10/3/036008.

[21] H. Fang, Y. Wang, and J. He, "Spiking Neural Networks for Cortical Neuronal Spike Train Decoding," *Neural Computation*, vol. 22, no. 4, pp. 1060–1085, Apr. 2010, doi: 10.1162/neco.2009.10-08-885.

[22] D. Ma *et al.*, "Darwin3: a large-scale neuromorphic chip with a novel ISA and on-chip learning," *National Science Review*, vol. 11, no. 5, p. nwae102, 2024.

[23] J. E. O'Doherty, M. M. Cardoso, J. G. Makin, and P. N. Sabes, "Nonhuman primate reaching with multichannel sensorimotor cortex electrophysiology," *Zenodo http://doi. org/10.5281/zenodo*, vol. 583331, 2017.

[24] B. P. Christie *et al.*, "Comparison of spike sorting and thresholding of voltage waveforms for intracortical brain–machine interface performance," *Journal of neural engineering*, vol. 12, no. 1, p. 016009, 2014.

[25] A. L. Hodgkin and A. F. Huxley, "A quantitative description of membrane current and its application to conduction and excitation in nerve," *The Journal of physiology*, vol. 117, no. 4, p. 500, 1952.

[26] A. N. Burkitt, "A review of the integrate-and-fire neuron model: I. Homogeneous synaptic input," *Biological cybernetics*, vol. 95, pp. 1–19, 2006.

[27] I.-M. Comşa, K. Potempa, L. Versari, T. Fischbacher, A. Gesmundo, and J. Alakuijala, "Temporal coding in spiking neural networks with alpha synaptic function: learning with backpropagation," *IEEE transactions on neural networks and learning systems*, vol. 33, no. 10, pp. 5939–5952, 2021.

[28] R. Hunger, *Floating point operations in matrix-vector calculus*, vol. 2019. Munich University of Technology, Inst. for Circuit Theory and Signal …, 2005.